



## FULL PAPER

# Hemilabile *N*-heterocyclic carbene and nitrogen ligands on Fe (II) catalyst for utilization of CO<sub>2</sub> into cyclic carbonate

Fei Chen<sup>1</sup> | Sheng Tao<sup>2</sup> | Ning Liu<sup>2</sup> | Cheng Guo<sup>3</sup> | Bin Dai<sup>1,2</sup>

<sup>1</sup>School of Chemical Engineering and Technology, Tianjin University, Tianjin, China

<sup>2</sup>School of Chemistry and Chemical Engineering, Key Laboratory for Green Processing of Chemical Engineering of Xinjiang Bingtuan, Shihezi University, Shihezi, China

<sup>3</sup>Cancer Institute, The Second Affiliated Hospital, Zhejiang University School of Medicine, Hangzhou, China

**Correspondence**

Ning Liu, School of Chemistry and Chemical Engineering, Key Laboratory for Green Processing of Chemical Engineering of Xinjiang Bingtuan, Shihezi University, North Fourth Road, Shihezi 832003, Xinjiang, China.  
Email: ningliu@shzu.edu.cn

Cheng Guo, Cancer Institute, The Second Affiliated Hospital, Zhejiang University School of Medicine, Hangzhou 310009, Zhejiang, China.  
Email: cheng\_guo@zju.edu.cn

Bin Dai, School of Chemical Engineering and Technology, Tianjin University, Tianjin 300072, China.  
Email: db\_tea@shzu.edu.cn

**Funding information**

Double First-Class Program of Shihezi University, Grant/Award Number: SHYL-ZD201801; International Partnership Program of Shihezi University, Grant/Award Number: GJHZ201908; Shihezi Young and Middle-Aged Leading Scientists Program, Grant/Award Number: 2019RC01; Xinjiang Bingtuan Young and Middle-Aged Leading Scientists Program, Grant/Award Number: 2020CB027; National Natural Science Foundation of China, Grant/Award Number: 21868033

Six Fe (II) complexes were synthesized based on the concept of the hemilability of hybrid ligands, and their catalytic behaviors and performances were evaluated for the fixation of CO<sub>2</sub> via the cycloaddition of epoxides. The catalytic potential of the Fe (II) complexes, in combination with bis(triphenylphosphoranylidene)ammonium chloride, have been proved to achieve the efficient conversion in some challenging substrates such as internal, disubstituted epoxides, oxetanes, and fatty acid-derived epoxides for synthesis of cyclic carbonates under the mild reaction conditions. Ultraviolet–visible and in situ Fourier transform infrared spectroscopy experiments as well as our previous coordination of Ni complexes studies revealed that the origin of activity of Fe (II) complexes might be attributed to the *trans* effect between *N*-heterocyclic carbene ligands and pyridine nitrogen donors.

**KEYWORDS**

carbon dioxide, catalyst design, cyclic carbonate, Fe catalysis, *Trans* effect

## 1 | INTRODUCTION

Carbon dioxide (CO<sub>2</sub>) is an abundant, nontoxic, and renewable C1 feedstock that provides an attractive alternative for organic synthesis from fossil fuel to sustainable resources.<sup>[1]</sup> The utilization of CO<sub>2</sub> as renewable C1 building block must overcome both the thermodynamic stability of CO<sub>2</sub> and its kinetic inertness.<sup>[1c]</sup> The synthesis of cyclic carbonates from CO<sub>2</sub> and epoxides is one of the most promising reaction route for the CO<sub>2</sub> utilization due to its high atomic economy.<sup>[2]</sup> Cyclic carbonates are important raw materials in chemical industry, which can be used for aprotic polar solvents, the preparation of polycarbonate, and ion carriers for lithium-based batteries.<sup>[1e]</sup> In the past few decades, hydrogen bond donor has represented an efficiently organocatalyzed strategy for the formation cyclic carbonates from CO<sub>2</sub> and epoxides.<sup>[3]</sup> Recently, nonnoble metal catalysts, including Al,<sup>[4]</sup> Co,<sup>[5]</sup> Cr,<sup>[6]</sup> Mn,<sup>[7]</sup> Mg,<sup>[8]</sup> Zn complexes,<sup>[9]</sup> and bimetallic complexes,<sup>[10]</sup> have showed promising application potentials for the utilization of CO<sub>2</sub>.

Fe is one of the particularly attractive metals because of its abundance on earth.<sup>[11]</sup> A wide range of Fe-based catalysts has been developed by Alhashmialameer et al.,<sup>[12]</sup> Seong et al.,<sup>[13]</sup> Della Monica et al.,<sup>[14]</sup> Whiteoak et al.,<sup>[15]</sup> Bucharth et al.,<sup>[16]</sup> Buonerba et al.,<sup>[17]</sup> and our group.<sup>[18]</sup> Nevertheless, high temperature, high CO<sub>2</sub> pressure, and limited scope of substrates remain impediments of these approaches. The design of ligands generally plays an important role in achieving efficiency and selectivity in the chemical transformation. The ligands with hybrid/different ligands generated the *trans* effect in catalytic process have attracted some attention in transition metal catalysis.<sup>[19]</sup> The difference of the coordination ability between the two ligands results in the weaker ligand preferring to dissociate from the metal center, which will provide one or more coordination sites for the activation of substrate molecule at metal center. Our group has successfully synthesized a variety of transition metal complexes bearing hybrid ligands such as Fe,<sup>[18,20]</sup> Pd,<sup>[21]</sup> Ru,<sup>[22]</sup> and Ni catalysts,<sup>[23]</sup> which have been given rise to unique and high reactivity in cycloaddition of CO<sub>2</sub>, coupling reaction, and oxidative reaction. In this work, we now report a simple, practical, and convenient synthetic procedure for Fe (II) complexes based on the *trans* effect between *N*-heterocyclic carbene (NHC) and nitrogen ligands. The Fe (II) complexes showed an extremely high activity for the cycloaddition of CO<sub>2</sub> and epoxides in mild conditions.

## 2 | EXPERIMENTAL SECTION

### 2.1 | General procedure for the synthesis of iron catalysts

The pyridine-bridge bidentate-type imidazolium salts were initially synthesized by the previous literature.<sup>[24]</sup> Imidazolium salts (0.5 mmol), Fe (acac)<sub>3</sub> (0.3 mmol), *t*-BuOK (0.5 mmol), and THF (3.0 ml) were put into 25-ml Schlenk tube. The Schlenk tube was subsequently heated to 65°C and reacted for 24 h. Then Schlenk tube was cooled to room temperature, the mixtures were filtered, the brown solid was collected, and then the desired products were isolated by flash chromatography.

#### 2.1.1 | Synthesis of iron complex 1a

3-Methyl-1-(pyridin-2-yl)-1*H*-benzo[*d*]imidazol-3-ium iodide (168.5 mg, 0.5 mmol), Fe (acac)<sub>3</sub> (106.0 mg, 0.3 mmol), and *t*-BuOK (56.1 mg, 0.5 mmol) were successfully added to a 25-ml Schlenk tube and dissolved in 3 ml of THF. The mixtures were subsequently heated to 65°C and reacted for 24 h. Then Schlenk tube was cooled to room temperature, the mixtures were filtered, the brown solid was collected, and then the desired products were isolated by flash chromatography (dichloromethane/methanol = 15:1). Brown powder (109.0 mg, yield 62%), mp = 206.8-207.2°C. <sup>1</sup>H NMR (400 MHz, DMSO-*d*<sub>6</sub>) δ 8.55-8.44 (m, 4H), 8.19-8.15 (m, 4H), 7.53-7.37 (m, 8H), 5.43 (s, 1H), 2.92-2.18 (m, 6H), 1.87 (s, 6H). HRMS (ESI) Calcd for C<sub>31</sub>H<sub>29</sub>FeIN<sub>6</sub>O<sub>2</sub> [M - I]<sup>+</sup> 573.1696. Found 573.1698. IR (neat, KBr): 1578, 1514, 1468, 1396, 1194, 1081, 773, 747 cm<sup>-1</sup>. The <sup>1</sup>H NMR spectra and FT-IR spectra of iron complex **1a** can be found in Figures S1 and S7.

#### 2.1.2 | Synthesis of iron complex 1b

3-Ethyl-1-(pyridin-2-yl)-1*H*-benzo[*d*]imidazol-3-ium iodide (175.5 mg, 0.5 mmol), Fe (acac)<sub>3</sub> (106.0 mg, 0.3 mmol), and *t*-BuOK (56.1 mg, 0.5 mmol) were successfully added to a 25-ml Schlenk tube and dissolved in 3 ml of THF. The mixtures were subsequently heated to 65°C and reacted for 24 h. Then Schlenk tube was cooled to room temperature, the mixtures was filtered, the brown solid was collected, and then the desired products were isolated by flash chromatography (dichloromethane/methanol = 15:1). Brown powder (100.1 mg, yield 55%), mp = 215.9-217.1°C. <sup>1</sup>H NMR (400 MHz, DMSO-*d*<sub>6</sub>) δ 8.56 (d, *J* = 8.0 Hz, 2H), 8.44

(d,  $J = 7.2$  Hz, 2H), 8.21 (t,  $J = 6.8$  Hz, 2H), 8.11 (d,  $J = 4.8$  Hz, 2H), 7.56 (d,  $J = 7.2$  Hz, 2H), 7.47-7.42 (m, 6H), 5.43 (s, 1H), 3.30-3.28 (m, 2H), 3.18-3.12 (m, 2H), 1.85 (s, 6H), 0.57 (t,  $J = 6.8$  Hz, 6H). HRMS (ESI) Calcd for  $C_{33}H_{33}FeIN_6O_2$   $[M - I]^+$  601.2009. Found 601.2005. IR (neat, KBr): 1578, 1514, 1477, 1405, 1245, 1190, 1093, 769, 744  $cm^{-1}$ . The  $^1H$  NMR spectra and FT-IR spectra of iron complex **1b** can be found in Figures S2 and S8.

### 2.1.3 | Synthesis of iron complex 1c

3-Propyl-1-(pyridin-2-yl)-1*H*-benzo[*d*]imidazol-3-ium iodide (182.5 mg, 0.5 mmol), Fe (acac)<sub>3</sub> (106.0 mg, 0.3 mmol), and *t*-BuOK (56.1 mg, 0.5 mmol) were successfully added to a 25-ml Schlenk tube and dissolved in 3 ml of THF. The mixtures were subsequently heated to 65°C and reacted for 24 h. Then Schlenk tube was cooled to room temperature, the mixtures were filtered, the brown solid was collected, and then the desired products were isolated by flash chromatography (dichloromethane/methanol = 15:1). Brown powder (113.4 mg, yield 60%), mp > 300°C.  $^1H$  NMR (400 MHz, DMSO-*d*<sub>6</sub>)  $\delta$  8.59 (d,  $J = 8.4$  Hz, 2H), 8.46 (d,  $J = 8.4$  Hz, 2H), 8.22 (d,  $J = 7.2$  Hz, 2H), 8.10-8.09 (m, 2H), 7.60 (d,  $J = 7.2$  Hz, 2H), 7.47-7.40 (m, 6H), 5.42 (s, 1H), 3.30-3.23 (m, 2H), 3.02-2.95 (m, 2H), 1.84 (s, 6H), 1.22-1.10 (m, 2H), 0.67-0.57 (m, 2H), 0.25 (t,  $J = 7.2$  Hz, 6H). HRMS (ESI) Calcd for  $C_{35}H_{37}FeIN_6O_2$   $[M - I]^+$  629.2322. Found 629.2323. IR (neat, KBr): 1573, 1510, 1472, 1405, 1346, 1274, 1181, 1017, 769, 744  $cm^{-1}$ . The  $^1H$  NMR spectra and FT-IR spectra of iron complex **1c** can be found in Figures S3 and S9.

### 2.1.4 | Synthesis of iron complex 1d

3-Butyl-1-(pyridin-2-yl)-1*H*-benzo[*d*]imidazol-3-ium iodide (189.5 mg, 0.5 mmol), Fe (acac)<sub>3</sub> (106.0 mg, 0.3 mmol), and *t*-BuOK (56.1 mg, 0.5 mmol) were successfully added to a 25-ml Schlenk tube and dissolved in 3 ml of THF. The mixtures were subsequently heated to 65°C and reacted for 24 h. Then Schlenk tube was cooled to room temperature, the mixtures were filtered, the brown solid was collected, and then the desired products were isolated by flash chromatography (dichloromethane/methanol = 20:1). Brown powder (127.4 mg, yield 65%), mp = 199.8-201.6°C.  $^1H$  NMR (400 MHz, DMSO-*d*<sub>6</sub>)  $\delta$  8.60-8.46 (m, 4H), 8.22-8.07 (m, 4H), 7.60-7.39 (m, 8H), 5.42 (s, 1H), 3.59-3.54 (m, 2H), 2.86-2.80 (m, 2H), 1.85 (s, 6H), 1.23-0.95 (m, 4H), 0.69-0.59 (m, 2H), 0.51-0.40 (m, 2H), 0.24 (t,  $J = 6.8$  Hz, 6H). HRMS (ESI) Calcd for  $C_{37}H_{41}FeIN_6O_2$   $[M - I]^+$

657.2635. Found 657.2636. IR (neat, KBr): 1573, 1510, 1468, 1409, 1354, 1270, 1181, 777, 744  $cm^{-1}$ . The  $^1H$  NMR spectra and FT-IR spectra of iron complex **1d** can be found in Figures S4 and S10.

### 2.1.5 | Synthesis of iron complex 1e

3-Pentyl-1-(pyridin-2-yl)-1*H*-benzo[*d*]imidazol-3-ium iodide (196.5 mg, 0.5 mmol), Fe (acac)<sub>3</sub> (106.0 mg, 0.3 mmol), and *t*-BuOK (56.1 mg, 0.5 mmol) were successfully added to a 25-ml Schlenk tube and dissolved in 3 ml of THF. The mixtures were subsequently heated to 65°C and reacted for 24 h. Then Schlenk tube was cooled to room temperature, the mixtures were filtered, the brown solid was collected, and then the desired products were isolated by flash chromatography (dichloromethane/methanol = 20:1). Brown powder (119.8 mg, yield 59%) mp = 210.7-212.4°C.  $^1H$  NMR (400 MHz, DMSO-*d*<sub>6</sub>)  $\delta$  8.60 (d,  $J = 8.4$  Hz, 2H), 8.47 (d,  $J = 7.2$  Hz, 2H), 8.22-8.18 (m, 2H), 8.09 (d,  $J = 5.6$  Hz, 2H), 7.60 (d,  $J = 7.2$  Hz, 2H), 7.48-7.39 (m, 6H), 5.40 (s, 1H), 3.64-3.57 (m, 2H), 2.85-2.78 (m, 2H), 1.83 (s, 6H), 1.07-1.02 (m, 2H), 0.68-0.34 (m, 16H).  $C_{39}H_{45}FeIN_6O_2$   $[M - I]^+$  685.2953. Found 685.2967. IR (neat, KBr): 1578, 1527, 1480, 1405, 1354, 1265, 1190, 1085, 1013, 764, 739  $cm^{-1}$ . The  $^1H$  NMR spectra and FT-IR spectra of iron complex **1e** can be found in Figures S5 and S11.

### 2.1.6 | Synthesis of iron complex 1f

5,6-Dimethyl-3-propyl-1-(pyridin-2-yl)-1*H*-benzo[*d*]imidazol-3-ium iodide (196.5 mg, 0.5 mmol), Fe (acac)<sub>3</sub> (106.0 mg, 0.3 mmol), and *t*-BuOK (56.1 mg, 0.5 mmol) were successfully added to a 25-ml Schlenk tube and dissolved in 3 ml of THF. The mixtures were subsequently heated to 65°C and reacted for 24 h. Then Schlenk tube was cooled to room temperature, the mixtures were filtered, the brown solid was collected, and then the desired products were isolated by flash chromatography (dichloromethane/methanol = 20:1). Brown powder (101.5 mg, yield 50%), mp = 230.9-232.2°C.  $^1H$  NMR (400 MHz, DMSO-*d*<sub>6</sub>)  $\delta$  8.57-8.55 (m, 2H), 8.25 (s, 2H), 8.19 (t,  $J = 7.6$  Hz, 2H), 8.09 (d,  $J = 7.6$  Hz, 2H), 7.40-7.37 (m, 4H), 5.40 (s, 1H), 3.27-3.20 (m, 2H), 2.93-2.85 (m, 2H), 2.44 (s, 6H), 2.33 (s, 6H), 1.83 (s, 6H), 1.17-1.12 (m, 2H), 0.59-0.56 (m, 2H), 0.22 (t,  $J = 7.2$  Hz, 6H). HRMS (ESI) Calcd for  $C_{39}H_{45}FeIN_6O_2$   $[M - I]^+$  685.2949. Found 685.2948. IR (neat, KBr): 1573, 1518, 1472, 1409, 1346, 1177, 1017, 756  $cm^{-1}$ . The  $^1H$  NMR spectra and FT-IR spectra of iron complex **1f** can be found in Figures S6 and S12.

## 2.2 | General procedure for the synthesis of cyclic carbonate

Epoxides (10.0 mmol), catalyst **1d** (0.03 mmol), and PPNCl (0.3 mmol) were successively added to a 25-ml stainless steel reactor that was equipped with a magnetic stirrer. The reactor was pressurized with CO<sub>2</sub> to 5 bar and heated to 50°C and reacted for 24 h. After the reaction, the stainless steel reactor was cooled to room temperature, and excess CO<sub>2</sub> was slowly vented off. The reaction mixtures were added to dichloromethane (2 × 10 ml). After the reaction, the mixture was concentrated under vacuum, and the cyclic carbonates were obtained by flash chromatography. Characterization data for cyclic carbonates can be found in the supporting information. NMR spectra of cyclic carbonate can be found in Figures S13–S58.

## 2.3 | Preparation of single crystals

The crystalline material was prepared via a layer-to-layer diffusion method. The Fe complex **1c** was added to the solution of dichloromethane (10 ml) and layered with hexane. After 2–3 days, a crystal suitable for single-crystal X-ray diffraction was obtained. Crystallographic data of the structures were deposited in the Cambridge Crystallographic Database Centre, supplementary publication No. CCDC 2007148 for Fe complex **1c**. X-ray data for Fe complex **1c** can be found in Figure S59.

## 2.4 | Analytical methods

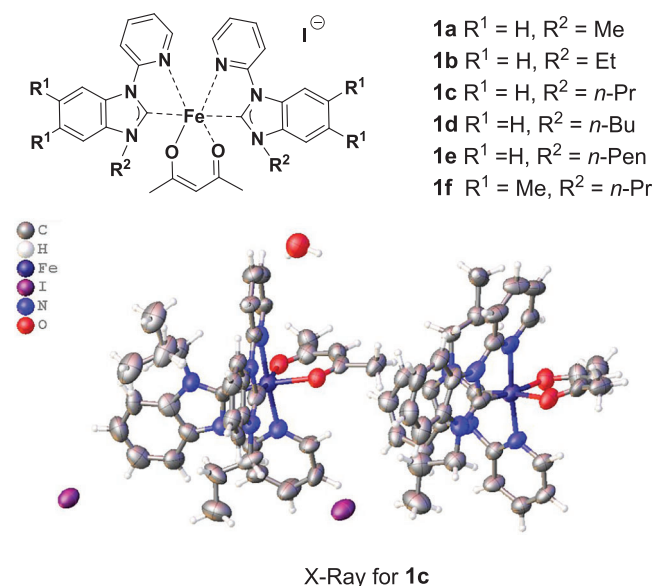
The NMR spectra were recorded on a Bruker Avance III HD 400 spectrometer using tetramethyl silane (TMS) as an internal standard (400 MHz for <sup>1</sup>H NMR and 100 MHz for <sup>13</sup>C NMR). HRMS data were collected on a Bruker ultrafleXtreme mass spectrometer. Single-crystal structure determination was conducted on a Bruker D8 Venture X-ray diffractometer equipped with a PHOTON II CPAD detector. UV–vis spectra of samples were obtained in solution using a MAPADA UV-6100 double beam UV–vis spectrophotometer. In situ FT-IR was collected on a Mettler Toledo ReactIR15, MCT detector analysis system. Gas chromatography (GC) analyses were carried on a Shimadzu GC-2014 equipped with a packed column (Stabilwax-DB, 30 m × 0.65 mm) using a flame ionization detector.

## 3 | RESULTS AND DISCUSSION

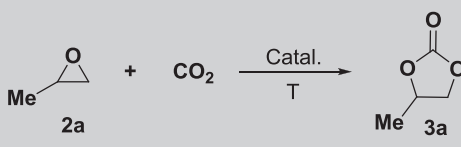
The bidentate-type imidazolium salts used as NHC precursors were prepared following the previous report.<sup>[24b]</sup>

Six Fe (II) complexes **1a–1f** (Scheme 1) were prepared through coordination reaction of imidazolium salts with Fe(acac)<sub>3</sub> in the presence of *t*-BuOK in THF under 65°C for 24 h. The Fe (II) complexes **1a–1f** were synthesized without the use of glove box or inert-atmosphere operation, and they were stable in the air. The molecule structure of Fe (II) complex **1c** was determined by the X-ray crystallography (Scheme 1). As depicted in Scheme 1, Fe (II) center coordinated with two pyridine bridged-carbene bidentate ligands and one acetylacetonate ligand with a noncoordinating iodine anions. The catalytic performance of six Fe (II) complexes **1a–1f** was evaluated in the synthesis of cyclic carbonates from CO<sub>2</sub> and epoxides.

Six Fe (II) complexes **1a–1f** were investigated in the cycloaddition of propylene oxide (PO) **2a** and CO<sub>2</sub> combination with a nucleophilic additive as cocatalysts (Table 1). First, the influence of alkyl chain lengths bearing Fe complexes on their catalytic performance was evaluated using TBAI as a nucleophilic additive. The results showed that the activity of the catalysts increased with lengthening of alkyl chain (Table 1, Entries 1–4); the activity keeps constant when lengthening of alkyl chain from *n*-butyl to *n*-pentyl (Table 1, Entries 4 vs. 5). The catalytic performance of different alkyl chain lengths is in the following order: *n*-pentyl ≈ *n*-butyl > *n*-propyl > ethyl > methyl (Table 1, Entries 1–5). The substituents at the phenyl ring on the catalytic performance were also investigated, suggesting that the substituents at the phenyl ring have a negligible influence on catalytic activity (Table 1, Entries 3 vs. 6). A series of nucleophilic additive, including TBAI, TBAB, TBAC, TBOAB, TBOAC, TBHSO<sub>4</sub>, and PPNCl in combination with Fe



**SCHEME 1** The Fe (II) complexes in this work

**TABLE 1** Optimization of propylene carbonate synthesis<sup>a</sup>


Entry	Catalyst (mmol)	Cocatalyst (mmol) <sup>b</sup>	T (°C)	Time (h)	P (bar)	Yield (%)
1	<b>1a</b> (0.03)	TBAI (0.3)	40	24	5	19
2	<b>1b</b> (0.03)	TBAI (0.3)	40	24	5	22
3	<b>1c</b> (0.03)	TBAI (0.3)	40	24	5	25
4	<b>1d</b> (0.03)	TBAI (0.3)	40	24	5	31
5	<b>1e</b> (0.03)	TBAI (0.3)	40	24	5	32
6	<b>1f</b> (0.03)	TBAI (0.3)	40	24	5	26
7	<b>1d</b> (0.03)	TBAI (0.3)	50	24	5	37
8	<b>1d</b> (0.03)	TBAB (0.3)	50	24	5	66
9	<b>1d</b> (0.03)	TBAC (0.3)	50	24	5	61
10	<b>1d</b> (0.03)	TBOAB (0.3)	50	24	5	69
11	<b>1d</b> (0.03)	TBOAC (0.3)	50	24	5	20
12	<b>1d</b> (0.03)	TBHSO <sub>4</sub> (0.3)	50	24	5	69
13	<b>1d</b> (0.03)	PPNCl (0.3)	50	24	5	92
14	<b>1d</b> (0.03)	PPNCl (0.03)	50	24	5	33
15	<b>1d</b> (0.03)	PPNCl (0.06)	50	24	5	34
16	<b>1d</b> (0.03)	PPNCl (0.09)	50	24	5	39
17	<b>1d</b> (0.03)	PPNCl (0.12)	50	24	5	40
18	<b>1d</b> (0.03)	PPNCl (0.15)	50	24	5	53
19	<b>1d</b> (0.03)	PPNCl (0.45)	50	24	5	94
20	<b>1d</b> (0.01)	PPNCl (0.1)	50	24	5	37
21	<b>1d</b> (0.02)	PPNCl (0.2)	50	24	5	54
22	<b>1d</b> (0.03)	PPNCl (0.06)	60	24	5	57
23	<b>1d</b> (0.03)	PPNCl (0.06)	70	24	5	61
24	<b>1d</b> (0.03)	PPNCl (0.06)	80	24	5	82
25	<b>1d</b> (0.03)	PPNCl (0)	50	24	5	23
26	<b>1d</b> (0)	PPNCl (0.3)	50	24	5	30
27	<b>1d</b> (0.03)	PPNCl (0.3)	50	24	2	49
28	<b>1d</b> (0.03)	PPNCl (0.3)	50	24	3	57
29	<b>1d</b> (0.03)	PPNCl (0.3)	50	24	4	72
30	<b>1d</b> (0.03)	PPNCl (0.3)	50	16	5	51
31	<b>1d</b> (0.03)	PPNCl (0.3)	50	20	5	80
32	<b>1d</b> (0.03)	PPNCl (0.3)	50	32	5	93

Abbreviations: PPNCl, bis(triphenylphosphoranylidene)ammonium chloride; TBAB, *tetra*-butylammonium bromide; TBAC, *tetra*-butylammonium chloride; TBAI, *tetra*-butylammonium iodide; TBHSO<sub>4</sub>, *tetra*-butylammonium hydrogen sulfate; TBOAB, *tetra*-octylammonium bromide; TBOAC, *tetra*-butylammonium acetate.

<sup>a</sup>Reaction conditions: PO (10.0 mmol), catalyst (indicated in Table 1), cocatalyst (indicated in Table 1), no solvent.

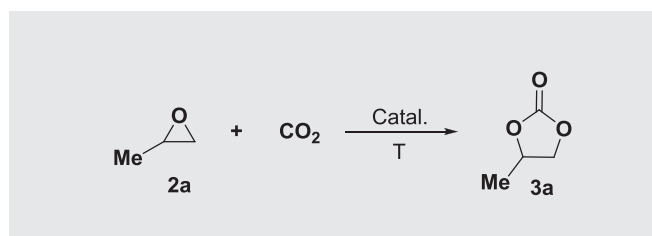
<sup>b</sup>Determined by GC using biphenyl as an internal standard.

(II) complex **1d** as catalyst, were also explored (Table 1, Entries 7–13). Binary systems both Fe (II) complex **1d**/PPNCl gave a better result with a 92% yield of product (Table 1, Entry 13), and Calo and coworkers<sup>[25]</sup> revealed that the bulkiness of the quaternary ammonium cation forces the chloride anion away from the cation, which rendered the counter anion more nucleophilic. Therefore, we infer that the energetic performance of PPNCl as a nucleophilic additive could be ascribed to the steric hindrance, which weakened electrostatic interaction between chloride anion and cation so as to promote the chloride more nucleophilic. Next, the effect of the different loading amount of the Fe complexes and PPNCl on the transformation was evaluated (Table 1, Entries 13–21). The results demonstrated that an Fe complex **1d**

loading amount of 0.3 mol%, together with PPNCl loading amount of 3 mol%, was the optimized conditions (Table 1, Entry 13). In order to explore the reason for the loading amount of PPNCl being 10 equiv to Fe complex **1e**, we also investigated the influence of temperature on the reaction under low loading amount of PPNCl. As indicated Table 1, when the reaction temperature increased to 80°C, an 82% yield was obtained even with low PPNCl loading of 0.6 mol% (Table 1, Entries 22–24). This might be explained that low temperature is difficult to trigger reaction with low concentration of PPNCl. The nucleophilic reagent (PPNCl) will achieve the ability for nucleophilic attack on the carbon atom of epoxides until the concentration of PPNCl reached a high concentration under relative reaction temperature. The control experiments in the presence of PPNCl or catalyst **1d** alone were also performed, confirming the essential nature of catalyst **1d** or PPNCl (Table 1, Entries 25 and 26). This clearly showed that the cooperative effect from catalyst **1d** and PPNCl was beneficial toward this reaction (Table 1, Entries 13 vs. 25 and 26). The influences of pressure of CO<sub>2</sub> (Table 1, Entries 13 and 27–29) and reaction time (Table 1, Entries 13 and 30–32) were explored, and it was demonstrated that a CO<sub>2</sub> pressure of 5 bar and reaction time of 24 h were the optimized conditions (Table 1, Entry 13).

Under the optimized conditions, a series of different terminal substrates were investigated, and the results were shown in Table 2. The epoxides bearing different

**TABLE 2** Scope of terminal substrates<sup>a</sup>

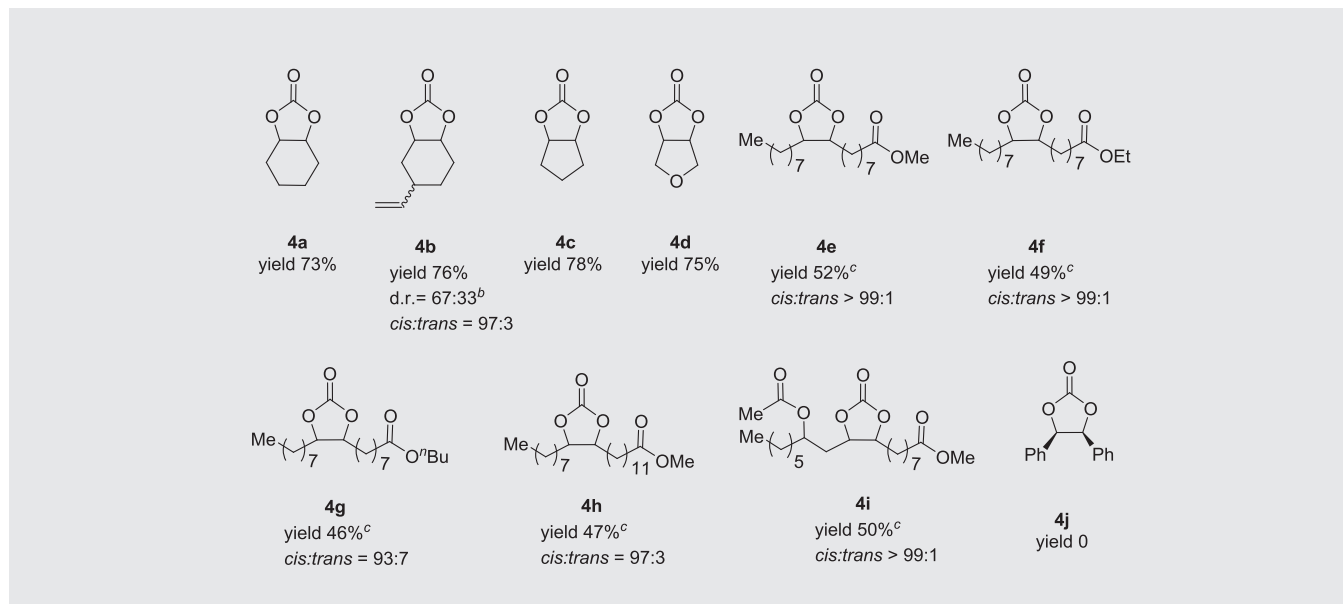


<sup>a</sup>Reaction conditions: epoxides (10 mmol), **1d** (0.030 mmol, 0.3 mol%), PPNCl (0.3 mmol, 3.0 mol%), neat, 50°C, 5 bar of CO<sub>2</sub>, 24 h, determined by isolated yields.

<sup>b</sup>80°C.

<sup>c</sup>80°C, 2-ml DMF.

**TABLE 3** Scope of internal substrates<sup>a</sup>



<sup>a</sup>Reaction conditions: epoxides (10 mmol), **1d** (0.030 mmol, 0.3 mol%), PPNCl (0.3 mmol, 3.0 mol%), neat, 80°C, 5 bar of CO<sub>2</sub>, 24 h, determined by isolated yields.

<sup>b</sup>The d.r. values and cis:trans ratio were determined by <sup>1</sup>H and <sup>13</sup>C NMR spectroscopy.

<sup>c</sup>100°C.

aliphatic chain length all achieved high product yields (Table 2, **3a–3d**). The results implied that the chain length bearing epoxides has a negative effect on the reactivity. Various functional groups bearing the terminal epoxides were tolerated, giving the desired products **3e–3k** in 83–95% yield at the 50°C and 5 bar of CO<sub>2</sub> in absence of the solvent. The 2,2-dimethyloxirane is also a challenging substrate due to the steric hindrance.<sup>[26]</sup> To our delight, the sterically hindered 2,2-dimethyloxirane **2l** was also successfully converted. The 63% yield of **3l** was obtained when the reaction was performed under 80°C. The fatty acid esters-based epoxies as a longer aliphatic chain substrates exhibited exceeding reactivity in our developed catalyzed system, affording the desired product of **3m** in 96% yield. The high conversion of this substrate required a DMF (*N,N*-dimethylformamide) as solvent because of its solid state (Table 2, **3n**).

Normally, the internal epoxides suffer low activity in cycloaddition reactions with CO<sub>2</sub> because of their high steric hindrance (Table 3).<sup>[18b,27]</sup> Next, the limitation and scope of the internal epoxides were investigated in the developed Fe-catalyzed system. Four bicyclic epoxides, such as two six-membered bicyclic cyclohexene oxide and cyclohexene oxide containing *exo*-cyclic double bonds, two five-membered bicyclic epoxides, could be converted into their cyclic carbonates **4a–4d** in good yields by increasing reaction temperature and prolonging time. The fatty acid esters are often more challenging substrates because of their high hindrance effect. Therefore, the limitation of the Fe-catalyzed system for the synthesis of fatty acid based biocarbonates was evaluated (Table 3). First, the reaction of epoxidized methyl oleate with CO<sub>2</sub> was performed, and a bio-based carbonate **4e** was obtained in a yield of 52%. Next, more epoxidized fatty acid esters, such as epoxidized ethyl oleate, epoxidized butyl oleate, epoxidized methyl erucate, and ricinoleic acid-derived epoxide, were also suitable for the cycloaddition reactions with CO<sub>2</sub>, giving moderate product yields (Table 3, **4f–4i**). At last, more bulky stilbene oxide was evaluated in the developed Fe catalytic system; however, no desired product was obtained (Table 3, **4j**).

In order to prove the interaction of the catalyst **1d** with substrate epichlorohydrin and cocatalyst PPnCl, we carried out UV-vis spectra titration experiments to investigate their interaction (Figure 1). Upon addition of epichlorohydrin to the acetonitrile solution of the catalyst **1d**, shifting of the characteristic peaks was observed from 266 and 311 cm<sup>-1</sup> to 259 and 316 cm<sup>-1</sup>, respectively (Figure 1). However, shifting of the characteristic peaks was not observed when PPnCl adding to the acetonitrile solution of the catalyst **1d**. These results suggested that the interaction between the catalyst **1d** and the epichlorohydrin might occur through the Fe center bearing the

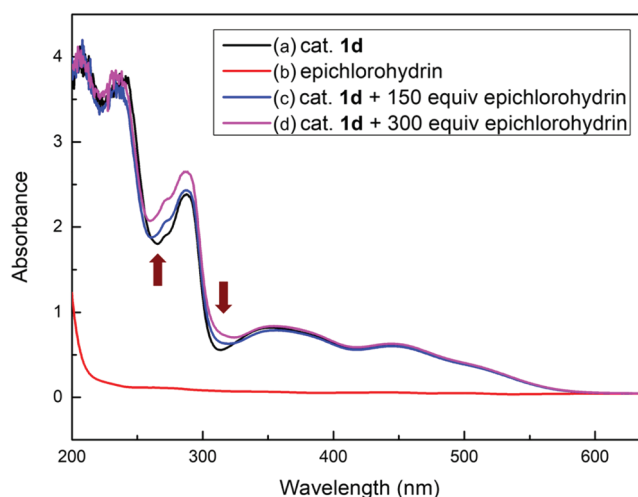


**FIGURE 1** Ultraviolet-visible (UV-vis) spectra on addition of epichlorohydrin to a solution of **1d** in CH<sub>3</sub>CN:

(a) catalyst **1d**  $\times 10^{-4}$  mol/L; (b) epichlorohydrin; (c) adding 150 equiv of epichlorohydrin to catalyst **1d** solution; (d) adding 300 equiv of epichlorohydrin to catalyst **1d** solution

catalyst **1d** coordinating with the oxygen atom of epichlorohydrin. Isosbestic points must be observed in the UV-vis titration experiments with 1:1 complexation between catalyst **1d** and epichlorohydrin. If there are no isosbestic points, two epichlorohydrins may coordinate with the catalyst **1d** or one of the ligands bearing the catalyst **1d** dissociated from Fe center. To explore the interaction between the catalyst **1d** and the epichlorohydrin, we performed the UV-vis titration experiments (see Figure S60 for details). The results indicated that no isosbestic points were observed in UV titration experiments. This suggested that two epoxides may coordinate with the Fe complex or one ligand dissociated from the Fe center. Our previous studies<sup>23</sup> revealed that two pyridine nitrogen ligands preferentially dissociated from metal center rather than an integral pyridine bridged-carbene bidentate ligands when the metal center needs to release two coordination sites; in other words, two carbene ligands always coordinate with the metal center. In addition, the catalyst **1d** will decompose after the reaction under the conditions that an integral pyridine bridged-carbene bidentate ligand dissociated from metal center. However, recovery experiment of the catalyst **1d** showed that 92% (average value of three experiments) of the catalyst **1d** recovered (see Figure S61 for details) after the reaction, which implied that the catalyst is stable in the process of catalytic cycle. The results above indicated that two pyridine nitrogen ligands bearing the catalyst **1d** temporarily dissociated from the metal center when the catalyst **1d** activated epichlorohydrins, thus ensuring the stability of the catalyst **1d**.

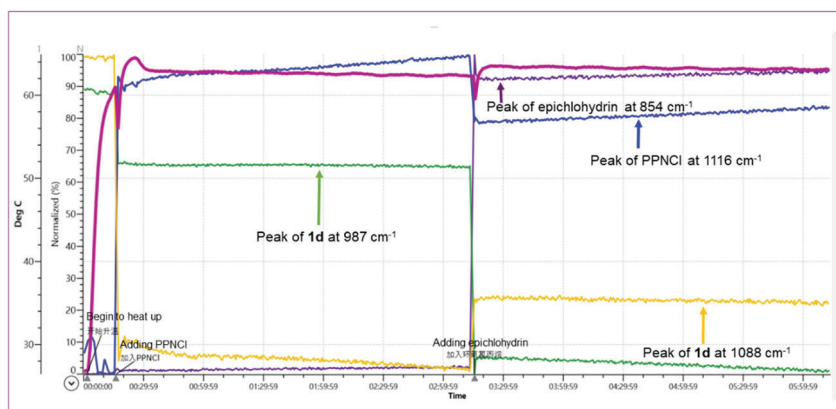
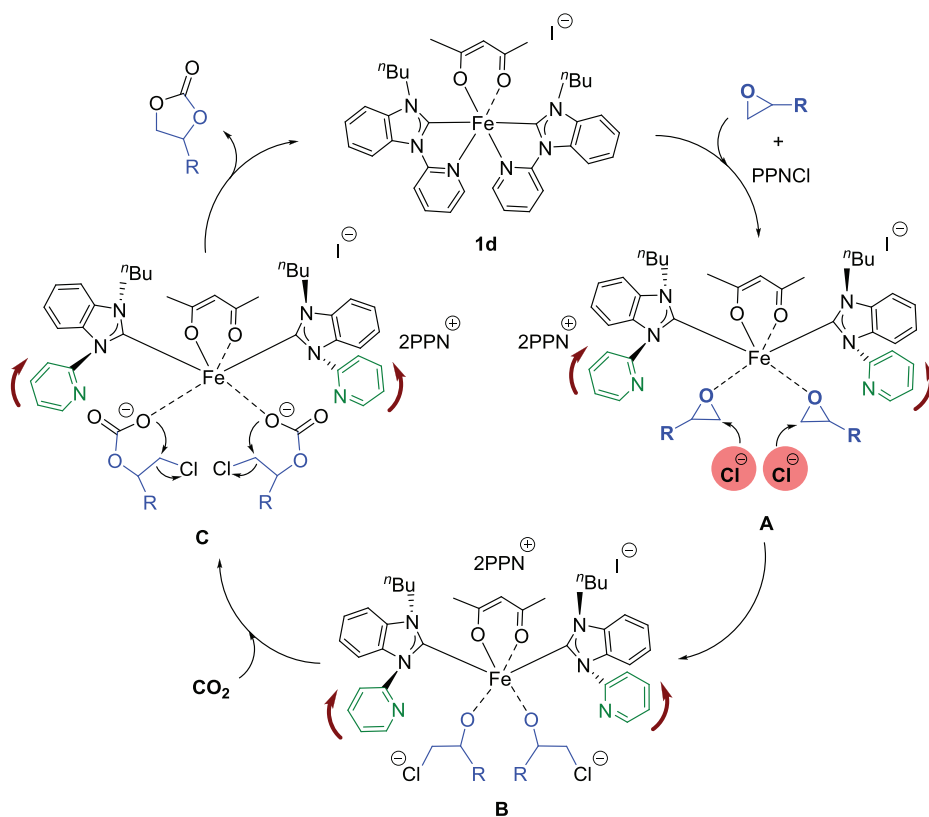


**FIGURE 2** In situ Fourier transform infrared spectroscopy (FT-IR) of Fe complex **1d** in 2 ml of acetonitrile solution (1 equiv, 0.02 mmol) upon the added of TBAB (15 equiv, 0.3 mmol) and epichlorohydrin (ECH) (500 equiv, 10 mmol), respectively, at 60°C

We performed a control experiment using in situ FT-IR spectra to study the interaction between **1d** and epichlorohydrin/PPNCI (Figure 2). Firstly, the catalyst **1d** was added to the 2 ml of acetonitrile solvent, and the absorption peak of the catalyst **1d** at 1088 (yellow line) and 987  $\text{cm}^{-1}$  (green line) was relatively stable with increasing of the reaction temperature (Figure 2). Upon the PPNCI was added to the acetonitrile solvent of the catalyst **1d**, the characteristic peak of **1d** at 1088 and 987  $\text{cm}^{-1}$  was unchanged, and the characteristic peak of PPNCI at 1116  $\text{cm}^{-1}$  (blue line) has a slight change during the addition of PPNCI to the catalyst system. The results are consistent with the experiments of UV-vis spectra, suggesting that the catalyst **1d** did not react with PPNCI.

Next, upon the epichlorohydrin was added to the mixture, the characteristic peak of **1d** at 987  $\text{cm}^{-1}$  (green line) was gradually weakened with prolonging the reaction time. The results are consistent with the experiments of UV-vis spectra, suggesting that the interaction between the catalyst **1d** and the epichlorohydrin was occurred. Our recent published work<sup>28</sup> reported the *trans* effect of cobalt complexes. In the report, we observed a characteristic absorption peak of IR for the acetylacetonate in situ FT-IR experiments for cobalt complexes, which supported the acetylacetonate preferring to dissociate from the cobalt center. While in this work, no characteristic absorption peak of IR for the acetylacetonate from in situ FT-IR experiments for iron complexes was observed (Figure 2). These



**SCHEME 2** The proposed mechanism for Fe (II) complexes catalyzed the cycloaddition of epoxide and  $\text{CO}_2$

results above suggested that the *trans* effect is not only related to the coordination ability of ligands but also depended on the electronic properties of metal.

The results of UV-vis and in situ FT-IR spectroscopy highlighted that the coordination environments of Fe complex **1d** have changed because of the *trans* effect between NHC and nitrogen ligands in the presence of the stimulation of substrates. Our previous works<sup>[23]</sup> have reported that the NHC ligands preferentially bind to the nickel atom than those containing nitrogen donors in the synthesis of nickel complexes, which revealed that nitrogen donors are preferred to dissociate from metal atom in comparison with NHC ligands. The spectroscopic measurements of UV-vis and in situ FT-IR as well as our previous research results suggested that Fe complex **1d** underwent leaving of pyridine ring due to the hemilability between NHC ligands and nitrogen donors, which provided two coordination sites for the activation of the epoxides with iron center to produce the intermediate **A** (Scheme 2). Previous literature<sup>[25]</sup> reported that both the size and structure of cations affect the nucleophilic ability of anions. Generally, the anion bearing the noncoordinating cation shows higher nucleophilicity than that of the coordinating cation.<sup>[29]</sup> In this work, the Fe complex **1d** contains a coordinating cation (Fe atom); however, PPNCl contains a noncoordinating cation. Therefore, the structure of the cations of Fe complex and PPNCl is completely different, which leads to their different nucleophilic ability. As shown in Table 1 (Entry 25), the use of Fe complex **1d** as one component catalyst in the absence of PPNCl led to a low yield. Therefore, the chlorine anion of PPNCl initiated the ring opening of the epoxide through the nucleophilic attack on the carbon of epoxide to produce an intermediate of **B**. A carbonyl insertion reaction of CO<sub>2</sub> to the intermediate **B** occurred and produced the intermediate **C**. Next, an intramolecular nucleophilic substitution of the intermediate **C** produced the desired products. During the breaking of C–O bond with the intermediate **C**, the pyridine nitrogen ligands re-coordinated with Fe center and regenerates the Fe catalyst **1d**.

## 4 | CONCLUSION

Iron complexes **1a–1f** based on the hemilability between NHC and pyridine nitrogen ligand were synthesized; their catalytic performance and the *trans* effect were investigated in the cycloaddition of epoxides and CO<sub>2</sub>. A variety of cyclic carbonates through the coupling of epoxides and epoxides with CO<sub>2</sub> were synthesized over an Fe-based catalytic system in combination of Fe complex **1d** with PPNCl. The Fe-based catalytic system allowed a wide range of substrates scope including the terminal

epoxides and internal epoxides as well as plant oil-based epoxides, affording desired cyclic carbonates in moderate to good yields. The catalytic system exhibited high catalytic performance with Fe complexes, which possessed the *trans* effect between NHC and pyridine nitrogen. In the substrates activation step, pyridine ring bearing Fe complexes preferred to dissociate from Fe center due to the competitive effect between NHC and pyridine nitrogen, which offered one coordination Fe sites for the activation of epoxides. After the reaction, the pyridine ring once again coordinated with the Fe center so as to stabilize the Fe active center. Therefore, the *trans* effect between NHC ligands and pyridine nitrogen plays an important role in regulating activity and stability of Fe catalysts to achieve a better balance. The knowledge obtained through these studies gains an understanding to the rational design and synthesis of transition-metal complexes for efficient chemical transformation.

## ACKNOWLEDGMENTS

We thank the support from the National Natural Science Foundation of China (21868033), Xinjiang Bingtuan Young and Middle-Aged Leading Scientists Program (2020CB027), Shihezi Young and Middle-Aged Leading Scientists Program (2019RC01), International Partnership Program of Shihezi University (GJHZ201908), and Double First-Class Program of Shihezi University (SHYL-ZD201801). We thank Ji-Xing Zhao for his assistance with the single-crystal X-ray diffraction, located at the Analysis and Testing Center, Shihezi University.

## AUTHOR CONTRIBUTIONS

**Fei Chen:** Conceptualization; data curation; formal analysis; investigation; methodology; software. **Sheng Tao:** Data curation; investigation; methodology; software. **Cheng Guo:** Conceptualization; data curation; formal analysis; methodology; software. **Bin Dai:** Conceptualization; data curation; investigation; methodology; supervision.

## CONFLICT OF INTEREST

The authors declare no competing financial interest.

## ORCID

Ning Liu  <https://orcid.org/0000-0001-7299-0400>

## REFERENCES

- [1] a) S. Wang, C. Xi, *Chem. Soc. Rev.* **2019**, *48*, 382. b) D. J. Darensbourg, *Chem. Rev.* **2007**, *107*, 2388. c) X.-B. Lu, D. J. Darensbourg, *Chem. Soc. Rev.* **2012**, *41*, 1462. d) M. Cokoja, C. Bruckmeier, B. Rieger, W. A. Herrmann, F. E. Kühn, *Angew. Chem., Int. Ed.* **2011**, *50*, 8510. e) A. Kleij, J. Rintjema, *Synthesis* **2016**, *48*, 3863. f) Q. Liu, L. Wu, R. Jackstell, M. Beller, *Nat.*

- Commun.* **2015**, *6*, 5933. g) J. Noh, J.-S. Chang, J.-N. Park, K. Y. Lee, S.-E. Park, *Appl. Organometal. Chem.* **2000**, *14*, 815.
- [2] a) A. Decortes, A. M. Castilla, A. W. Kleij, *Angew. Chem., Int. Ed.* **2010**, *49*, 9822. b) J. W. Comerford, I. D. V. Ingram, M. North, X. Wu, *Green Chem.* **2015**, *17*, 1966. c) Y. Yuan, Y. Xie, D. Song, C. Zeng, S. Chaemchuen, C. Chen, F. Verpoort, *Appl. Organometal. Chem.* **2017**, *31*, 3867.
- [3] a) M. Alves, B. Grignard, R. Mereau, C. Jerome, T. Tassaing, C. Detrembleur, *Catal. Sci. Technol.* **2017**, *7*, 2651. b) B.-H. Xu, J.-Q. Wang, J. Sun, Y. Huang, J.-P. Zhang, X.-P. Zhang, S.-J. Zhang, *Green Chem.* **2015**, *17*, 108. c) M. Cokoja, M. E. Wilhelm, M. H. Anthofer, W. A. Herrmann, F. E. Kühn, *ChemSusChem* **2015**, *8*, 2436. d) S. Sopeña, E. Martin, E. C. Escudero-Adán, A. W. Kleij, *ACS Catal.* **2017**, *7*, 3532. e) N. Liu, Y.-F. Xie, C. Wang, S.-J. Li, D. Wei, M. Li, B. Dai, *ACS Catal.* **2018**, *8*, 9945.
- [4] a) J. Rintjema, R. Epping, G. Fiorani, E. Martin, E. C. Escudero-Adán, A. W. Kleij, *Angew. Chem., Int. Ed.* **2016**, *55*, 3972. b) Y. Kim, K. Hyun, D. Ahn, R. Kim, M. H. Park, Y. Kim, *ChemSusChem* **2019**, *12*, 4211.
- [5] a) X. Jiang, F. Gou, F. Chen, H. Jing, *Green Chem.* **2016**, *18*, 3567. b) W.-M. Ren, G.-P. Wu, F. Lin, J.-Y. Jiang, C. Liu, Y. Luo, X.-B. Lu, *Chem. Sci.* **2012**, *3*, 2094. c) H. Ullah, B. Mousavi, H. A. Younus, Z. A. K. Khattak, S. Chaemchuen, S. Suleman, F. Verpoort, *Commun. Chem.* **2019**, *2*.
- [6] J. A. Castro-Osma, K. J. Lamb, M. North, *ACS Catal.* **2016**, *6*, 5012.
- [7] J. L. S. Milani, A. M. Meireles, W. A. Bezerra, D. C. S. Martins, D. Cangussu, R. P. das Chagas, *ChemCatChem* **2019**, *11*, 4393.
- [8] a) T. Ema, Y. Miyazaki, J. Shimonishi, C. Maeda, J.-y. Hasegawa, *J. Am. Chem. Soc.* **2014**, *136*, 15270. b) C. Maeda, T. Taniguchi, K. Ogawa, T. Ema, *Angew. Chem., Int. Ed.* **2015**, *54*, 134.
- [9] a) R. Ma, L.-N. He, Y.-B. Zhou, *Green Chem.* **2016**, *18*, 226. b) S. He, F. Wang, W.-L. Tong, S.-M. Yiu, M. C. W. Chan, *Chem. Commun.* **2016**, *52*, 1017. c) X. Jiang, F. Gou, X. Fu, H. Jing, *J. CO<sub>2</sub> Util.* **2016**, *16*, 264.
- [10] a) M. W. Lehenmeier, C. Bruckmeier, S. Klaus, J. E. Dengler, P. Deglmann, A.-K. Ott, B. Rieger, *Chem. – Eur. J.* **2011**, *17*, 8858. b) M. North, C. Young, *ChemSusChem* **2011**, *4*, 1685. c) F. Della Monica, S. V. C. Vummaleti, A. Buonerba, A. D. Nisi, M. Monari, S. Milione, A. Grassi, L. Cavallo, C. Capacchione, *Adv. Synth. Catal.* **2016**, *358*, 3231. d) J. A. Castro-Osma, M. North, W. K. Offermans, W. Leitner, T. E. Müller, *ChemSusChem* **2016**, *9*, 791.
- [11] K. S. Egorova, V. P. Ananikov, *Angew. Chem., Int. Ed.* **2016**, *55*, 12150.
- [12] D. Alhashmialameer, J. Collins, K. Hattenhauer, F. M. Kerton, *Catal. Sci. Technol.* **2016**, *6*, 5364.
- [13] a) E. Y. Seong, J. H. Kim, N. H. Kim, K. H. Ahn, E. J. Kang, *ChemSusChem* **2019**, *12*, 409. b) N. H. Kim, E. Y. Seong, J. H. Kim, S. H. Lee, K.-H. Ahn, E. J. Kang, *J. CO<sub>2</sub> Util.* **2019**, *34*, 516.
- [14] F. Della Monica, B. Maity, T. Pehl, A. Buonerba, A. De Nisi, M. Monari, A. Grassi, B. Rieger, L. Cavallo, C. Capacchione, *ACS Catal.* **2018**, *8*, 6882.
- [15] C. J. Whiteoak, E. Martin, M. M. Belmonte, J. Benet-Buchholz, A. W. Kleij, *Adv. Synth. Catal.* **2012**, *354*, 469.
- [16] A. Buchard, M. R. Kember, K. G. Sandeman, C. K. Williams, *Chem. Commun.* **2011**, *47*, 212.
- [17] a) A. Buonerba, A. De Nisi, A. Grassi, S. Milione, C. Capacchione, S. Vagin, B. Rieger, *Catal. Sci. Technol.* **2015**, *5*, 118. b) J. E. Dengler, M. W. Lehenmeier, S. Klaus, C. E. Anderson, E. Herdtweck, B. Rieger, *Eur. J. Inorg. Chem.* **2011**, *2011*, 336.
- [18] a) F. Chen, N. Liu, B. Dai, *ACS Sustainable Chem. Eng.* **2017**, *5*, 9065. b) F. Chen, Q.-C. Zhang, D. Wei, Q. Bu, B. Dai, N. Liu, *J. Org. Chem.* **2019**, *84*, 11407.
- [19] a) P. Braunstein, F. Naud, *Angew. Chem., Int. Ed.* **2001**, *40*, 680. b) W. D. Bailey, L. Luconi, A. Rossin, D. Yakhvarov, S. E. Flowers, W. Kaminsky, R. A. Kemp, G. Giambastiani, K. I. Goldberg, *Organometallics* **2015**, *34*, 3998. c) A. Fleckhaus, A. H. Mousa, N. S. Lawal, N. K. Kazemifar, O. F. Wendt, *Organometallics* **2015**, *34*, 1627.
- [20] F. Chen, M. Li, J. Wang, B. Dai, N. Liu, *J. CO<sub>2</sub> Util.* **2018**, *28*, 181.
- [21] S. Tao, C. Guo, N. Liu, B. Dai, *Organometallics* **2017**, *36*, 4432.
- [22] C.-B. Bo, Q. Bu, X. Li, G. Ma, D. Wei, C. Guo, B. Dai, N. Liu, *J. Org. Chem.* **2020**, *85*, 4324.
- [23] Y.-B. Wang, B.-Y. Liu, Q. Bu, B. Dai, N. Liu, *Adv. Synth. Catal.* **2020**, *362*, 2930.
- [24] a) L. Wang, N. Liu, B. Dai, H. Hu, *Eur. J. Org. Chem.* **2014**, *2014*, 6493. b) F. Chen, D. Chen, L. Shi, N. Liu, B. Dai, *J. CO<sub>2</sub> Util.* **2016**, *16*, 391.
- [25] V. Caló, A. Nacci, A. Monopoli, A. Fanizzi, *Org. Lett.* **2002**, *4*, 2561.
- [26] F. Della Monica, A. Buonerba, V. Paradiso, S. Milione, A. Grassi, C. Capacchione, *Adv. Synth. Catal.* **2019**, *361*, 283.
- [27] a) L. Longwitz, J. Steinbauer, A. Spannenberg, T. Werner, *ACS Catal.* **2018**, *8*, 665. b) L. Peña Carrodeguas, À. Cristòfol, J. M. Fraile, J. A. Mayoral, V. Dorado, C. I. Herreras, A. W. Kleij, *Green Chem.* **2017**, *19*, 3535. c) N. Tenhumberg, H. Büttner, B. Schäffner, D. Kruse, M. Blumenstein, T. Werner, *Green Chem.* **2016**, *18*, 3775. d) H. Bittner, J. Steinbauer, T. Werner, *ChemSusChem* **2015**, *8*, 2655. e) C. Maeda, J. Shimonishi, R. Miyazaki, J. Hasegawa, T. Ema, *Chem. – Eur. J.* **2016**, *22*, 6556. f) J. Steinbauer, A. Spannenberg, T. Werner, *Green Chem.* **2017**, *19*, 3769. g) C. Miceli, J. Rintjema, E. Martin, E. C. Escudero-Adán, C. Zonta, G. Licini, A. W. Kleij, *ACS Catal.* **2017**, *7*, 2367. h) T. Ema, M. Yokoyama, S. Watanabe, S. Sasaki, H. Ota, K. Takaishi, *Org. Lett.* **2017**, *19*, 4070. i) Y. Hu, J. Steinbauer, V. Stefanow, A. Spannenberg, T. Werner, *ACS Sustainable Chem. Eng.* **2019**, *7*, 13257. j) K. Grollier, N. D. Vu, K. Onida, A. Akhdar, S. Norsic, F. D'Agosto, C. Boisson, N. Duguet, *Adv. Synth. Catal.* **2020**, *362*, 1696.
- [28] W.-Y. Song, Q. Liu, Q. Bu, D. Wei, B. Dai, N. Liu, *Organometallics* **2020**, *39*, 3546.
- [29] Y. Qin, H. Guo, X. Sheng, X. Wang, F. Wang, *Green Chem.* **2015**, *17*, 2853.

## SUPPORTING INFORMATION

Additional supporting information may be found online in the Supporting Information section at the end of this article.

**How to cite this article:** Chen F, Tao S, Liu N, Guo C, Dai B. Hemilabile *N*-heterocyclic carbene and nitrogen ligands on Fe (II) catalyst for utilization of CO<sub>2</sub> into cyclic carbonate. *Appl Organomet Chem.* 2020;e6099. <https://doi.org/10.1002/aoc.6099>